

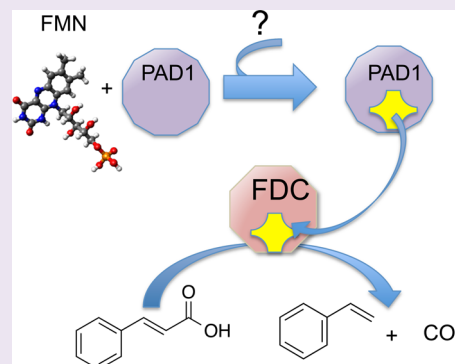
Isofunctional Enzymes PAD1 and UbiX Catalyze Formation of a Novel Cofactor Required by Ferulic Acid Decarboxylase and 4-Hydroxy-3-polyprenylbenzoic Acid Decarboxylase

Fengming Lin,^{†,‡,||} Kyle L. Ferguson,[†] David R. Boyer,[†] Xiaoxia Nina Lin,^{*,‡} and E. Neil G. Marsh^{*,†,§}

[†]Department of Chemistry, [‡]Department of Chemical Engineering, and [§]Department of Biological Chemistry, University of Michigan, Ann Arbor, Michigan 48109, United States

ABSTRACT: The decarboxylation of antimicrobial aromatic acids such as phenylacrylic acid (cinnamic acid) and ferulic acid by yeast requires two enzymes described as phenylacrylic acid decarboxylase (PAD1) and ferulic acid decarboxylase (FDC). These enzymes are of interest for various biotechnological applications, such as the production of chemical feedstocks from lignin under mild conditions. However, the specific role of each protein in catalyzing the decarboxylation reaction remains unknown. To examine this, we have overexpressed and purified both PAD1 and FDC from *E. coli*. We demonstrate that PAD1 is a flavin mononucleotide (FMN)-containing protein. However, it does *not* function as a decarboxylase. Rather, PAD1 catalyzes the formation of a novel, diffusible cofactor required by FDC for decarboxylase activity. Coexpression of FDC and PAD1 results in the production of FDC with high levels cofactor bound. Holo-FDC catalyzes the decarboxylation of phenylacrylic acid, coumaric acid and ferulic acid with apparent k_{cat} ranging from 1.4–4.6 s⁻¹.

The UV-visible and mass spectra of the cofactor indicate that it appears to be a novel, modified form of reduced FMN; however, its instability precluded determination of its structure. The *E. coli* enzymes UbiX and UbiD are related by sequence to PAD1 and FDC respectively and are involved in the decarboxylation of 4-hydroxy-3-octaprenylbenzoic acid, an intermediate in ubiquinone biosynthesis. We found that endogenous UbiX can also activate FDC. This implies that the same cofactor is required for decarboxylation of 4-hydroxy-3-polyprenylbenzoic acid by UbiD and suggests a wider role for this cofactor in metabolism.



Enzyme-catalyzed decarboxylation constitutes an important class of biological reactions that are ubiquitous in both primary and secondary metabolism. However, decarboxylation reactions are generally associated with high-energy barriers to reaction because the transition state involves a buildup of negative charge on the α -carbon. Nature has therefore evolved decarboxylases that employ a wide variety of catalytic strategies to facilitate decarboxylation using cofactors such as pyridoxal phosphate and thiamin pyrophosphate that serve as electron sinks and Lewis acidic metal ions.^{1–3}

Decarboxylases are also of interest for their potential use as industrial catalysts in the synthesis of optically pure intermediates for organic synthesis under mild reaction conditions.⁴ They have also been used in fermentation processes to produce short-chain alcohols and in the conversion of amino acids to chemical feedstocks such as styrene and acrylamide.^{5–7} One such enzyme is ferulic acid decarboxylase (FDC) from *Saccharomyces cerevisiae* that has been used in conjunction with phenylalanine ammonia lyase to engineer an *E. coli* strain capable of producing styrene from endogenous produced phenylalanine.⁸

FDC is found in various strains of yeast that detoxify antimicrobial compounds commonly used as food preservatives and flavorings, such as sorbic acid and cinnamic acid (phenylacrylic acid), by decarboxylation to yield CO₂ and the

volatile biproducts pentadiene and styrene.⁹ Genetic analysis established that two gene products are necessary for the metabolism of cinnamic acid to styrene (Figure 1); these were

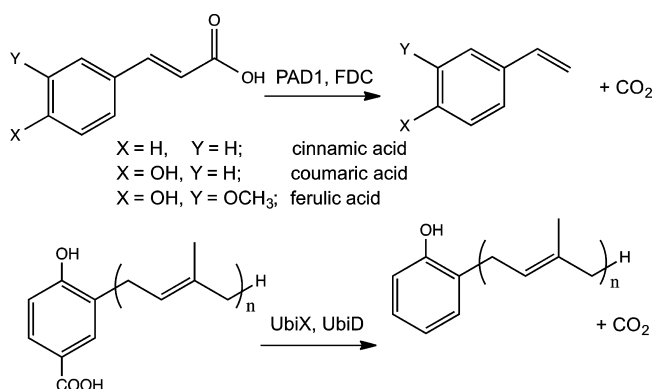


Figure 1. Decarboxylation reactions catalyzed by PAD1/FDC in yeast and the related decarboxylation catalyzed by UbiX/UbiD in bacteria as part of ubiquinone biosynthesis.

Received: October 7, 2014

Accepted: January 20, 2015

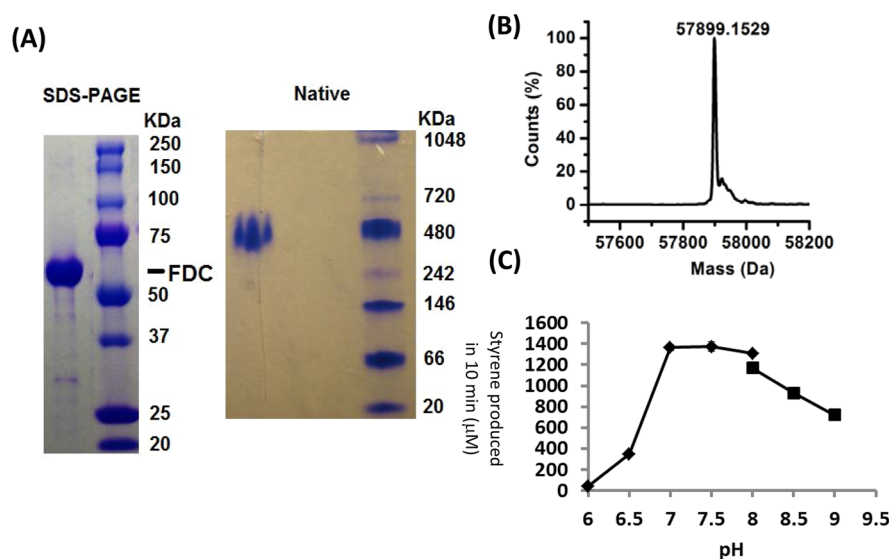


Figure 2. Purification and initial characterization of FDC. (A) SDS-PAGE and native PAGE analysis of purified FDC. (B) LC-ESI-MS analysis of purified FDC. (C) pH dependence of cinnamic acid decarboxylase activity; for assay details, see the main text. The buffers used were pH 6.0–8.0, 50 mM potassium phosphate buffer, 100 mM NaCl and pH 8.0–9.0, 50 mM Tris/Cl, 100 mM NaCl.

designated *PAD1* and *FDC* for phenylacrylic acid decarboxylase and ferulic acid decarboxylase, respectively.^{9–11} (Note that the term PAD is also used in the literature as an abbreviation for phenolic acid decarboxylase,^{4,7} leading to confusion between the two enzymes. However, whereas phenolic acid decarboxylase, which requires no cofactors for activity, catalyzes the decarboxylation of variously substituted phenolic acrylic acids, it does not catalyze the decarboxylation of phenylacrylic acid.) Interestingly, the *PAD1* and *FDC* genes were found to be homologous to *ubiX* and *ubiD* respectively, two genes involved in the biosynthesis of ubiquinone in a wide range of bacteria^{12–14} where they are involved in the decarboxylation of the aromatic intermediate 4-hydroxy-3-octaprenylbenzoic acid to 2-octaprenylphenol (Figure 1). However, how *FDC*/*PAD1* and *UbiD*/*UbiX* function together to effect these decarboxylation reactions remain unknown.

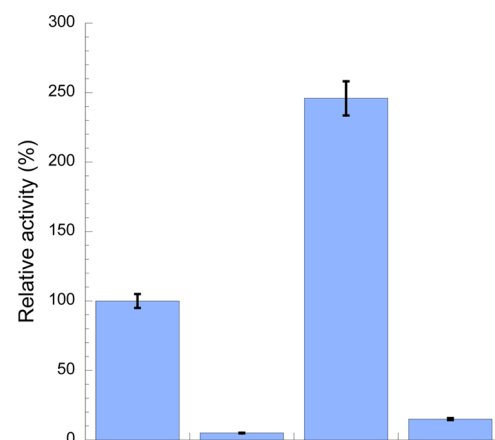
Sequence comparisons have suggested that both *UbiX* and *UbiD*, and by extension *PAD1* and *FDC*, may be flavin-containing proteins,^{15,16} but the role of this redox cofactor in the decarboxylation reaction remains unexplained. Here, we report the initial biochemical characterization of *PAD1* and *FDC*. We provide evidence that *PAD1* and *FDC* comprise a two-component system in which *PAD1* synthesizes a novel cofactor used by *FDC*. This cofactor is probably a covalently modified derivative of reduced flavin mononucleotide (FMN). Our results suggest that *UbiX* and *UbiD* constitute a similar two-component decarboxylase system and that the same flavin-based cofactor is necessary for the biosynthesis of ubiquinone.

RESULTS AND DISCUSSION

Properties of *S. cerevisiae* FDC Recombinantly Expressed in *E. coli*. FDC containing an N-terminal 6-histidine tag was successfully overexpressed in *E. coli* BL21 and purified to homogeneity by standard methods utilizing affinity chromatography on a nickel-NTA column (Figure 2A). The molecular weight of the enzyme as determined by LC-ESI-MS was 57898.15 ± 0.5 Da (Figure 2B), in excellent agreement with the predicted mass of 57897.8 Da. Analysis of FDC by native gel electrophoresis (Figure 2A) indicated that the

protein migrated with an apparent molecular weight of ~ 480 kDa, suggesting that the native protein adopts an oligomeric structure in solution. Interestingly, FDC purified from *E. coli* was active in the absence of *PAD1*, consistent with previous studies that found styrene production from engineered *E. coli* cells did not require the introduction of the *PAD1* gene.⁸ The enzyme activity was optimal between pH 7.0 and 8.0 (Figure 2C) and decreased sharply below pH 7.0.

The specific activity of FDC at pH 8.0 as determined by the GC-MS assay described in Methods was $\sim 0.54 \mu\text{mol styrene} \cdot \text{min}^{-1} \cdot \text{mg}^{-1}$ enzyme. Unexpectedly, it was found that dialyzing FDC against buffer (membrane cutoff = 3.5 kDa) for 24 h resulted in almost complete loss of activity (Figure 3), suggesting that FDC required a low molecular weight cofactor



FDC as isolated	+	-	-	-
FDC dialyzed	-	+	+	+
BL21 cell lysate	-	-	+	-
BL21 cell lysate dialyzed	-	-	-	+

Figure 3. Effect of dialysis and addition of *E. coli* BL21 cell lysate on FDC activity. The activity of FDC as purified from *E. coli* BL21 is arbitrarily assigned as 100% and corresponds to a specific activity of $\sim 0.54 \mu\text{mol styrene} \cdot \text{min}^{-1} \cdot \text{mg}^{-1}$ enzyme.

for activity. Consistent with this, addition of a cell-free lysate of *E. coli* BL21 was able to completely rescue activity (Figure 3). However, if the cell-free lysate was first dialyzed against buffer through a 3.5 kDa cutoff membrane, its ability to activate FDC was lost. Attempts to activate FDC using commonly encountered, commercially available biochemical cofactors, including thiamine pyrophosphate, pyridoxal phosphate, nucleotides, NADH, NADPH, FMN, and FAD, and various metal ions were unsuccessful.

UbiX Substitutes for PAD1 in *E. coli*. Both FDC and PAD1 are reported to be essential for the decarboxylation of phenylacrylic acid *in vivo* in *S. cerevisiae*;⁹ therefore, we considered whether the homologous *E. coli* protein, UbiX, was substituting for PAD1 in *E. coli*. To test this, we disrupted the *ubiX* gene in *E. coli* BL21 to create an *E. coli* BL21/ Δ *ubiX* strain. Expression and purification of FDC from the Δ *ubiX* strain resulted in protein completely lacking in decarboxylase activity and cell lysates prepared from this strain were unable to reactivate dialyzed FDC (Figure 4). However, the inactive

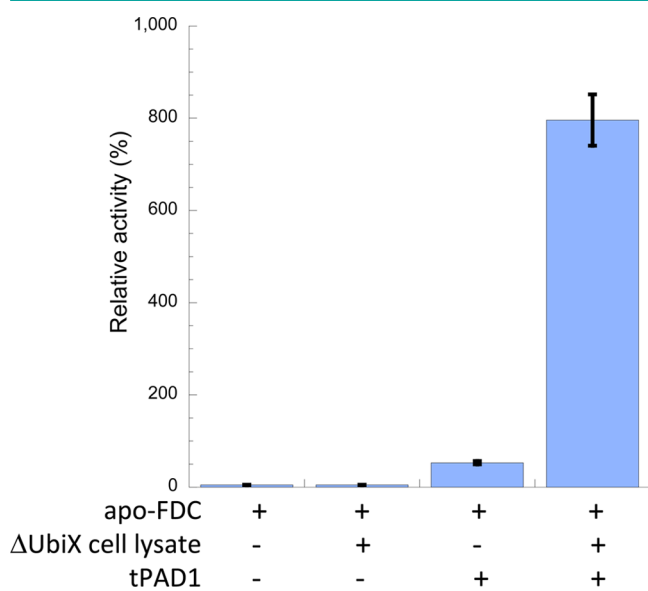


Figure 4. Role of tPAD1 in activation of apo-FDC purified from *E. coli* BL21/ Δ *ubiX*. Incubation of inactive, apo-FDC with *E. coli* BL21/ Δ *ubiX* cell lysates and tPAD1 activates the enzyme. The activity of FDC as purified from *E. coli* BL21 is arbitrarily assigned as 100% (column 1 Figure 3).

enzyme could be activated by lysates prepared from either wild-type *E. coli* BL21 or by lysates prepared from *E. coli* BL21/ Δ *ubiX* when purified PAD1 (lacking the N-terminal mitochondrial targeting sequence, as discussed below) was also added (Figure 4). These observations suggested that PAD1 and UbiX might function to synthesize a low molecular weight cofactor necessary for the activity of FDC.

Expression and Characterization of PAD1 in *E. coli*. To obtain a better understanding of the role of PAD1 in activating FDC, we overexpressed and purified this enzyme from *E. coli*. Initial attempts to express the full-length PAD1 in *E. coli* resulted in poor levels of expression and the recombinant protein lacked the expected FMN cofactor. However, deletion of the first 58 residues, which appear to encode a mitochondrial targeting sequence, resulted in the expression of soluble protein that could be purified by standard methods utilizing an N-terminal-encoded 6-histidine tag and affinity chromatography

on a nickel-NTA column (Figure 5A). The truncated form of PAD1 is designated tPAD1. The molecular weight of the protein determined by LC-ESI-MS was 21808.6 Da (Figure 5B), in excellent agreement with the predicted molecular weight of 21808.4 Da. The molecular weight of the native protein was estimated as ~300 kDa by gel filtration chromatography (data not shown), indicating that it is an oligomeric protein in solution.

Purified tPAD1 was yellow and the UV-visible spectrum exhibited maxima at 384 and 458 nm, characteristic of oxidized FMN (Figure 5C). The presence of FMN was confirmed by LC-ESI-MS. FMN was released from tPAD1 by precipitation of the protein with 1:1 dichloromethane/methanol, and subsequent chromatographic analysis of the supernatant identified a molecule with ($m+H^+$)/ z of 457.1 Da (Figure 5D) matching an authentic standard of FMN, $M_r = 456$. Interestingly, the absorption maximum at 384 nm is more intense than that at 458 nm, (Figure 5C) whereas for oxidized FMN the opposite is true. This suggested that tPAD1 may contain another chromophore, although no other molecules were identified by LC-ESI-MS. tPAD1 was unable to catalyze the conversion of cinnamic acid to styrene, demonstrating that, contrary to initial genetic analyses,¹⁰ the enzyme is not an isofunctional enzyme with FDC.

The crystal structures of *E. coli* O157:H7 Pad1p¹⁶ and *Pseudomonas aeruginosa* UbiX¹⁷ have been determined, revealing them to be a dodecameric proteins containing FMN. This is consistent with our characterization of PAD1 as an FMN-containing protein that exists as large oligomers in solution and suggests a common structure and function for these proteins. Interestingly, Pad1p and UbiX are structurally related to the family of flavin-dependent peptidyl cysteine decarboxylases. These include EpiD and MrsD, for which structures have been determined,^{18,19} that are involved in the biosynthesis of the lantibiotic peptides epidermin and mersacidin, respectively,²⁰ and Dpf that catalyzes the decarboxylation of 4'-phospho-N-pantothenoyl-cysteine to 4'-phospho-N-pantetheine in coenzyme A biosynthesis.^{21–23} However, there is currently no evidence to support either Pad1p or PAD1 functioning as cysteinyl decarboxylases. Instead, as discussed below, our results suggest these enzymes are more likely involved in catalyzing the formation of a modified form of FMN.

Role of tPAD1 in Activation of FDC. To examine whether a direct interaction between FDC and PAD1 is necessary for the activation of FDC, the following experiment was performed. A dialysis cell was set up in which 1 μ M apo-FDC was introduced on one side of a 3.5 kDa cutoff dialysis membrane in a buffer containing 6.7 mM cinnamic acid. On the other side of the membrane purified tPAD1 and/or cell lysates of either *E. coli* BL21 or *E. coli* BL21/ Δ *ubiX* were introduced. At various times, the reaction was analyzed for the production of styrene by GC-MS (Figure 6). Whereas *E. coli* Δ *ubiX* cell lysate was unable to activate FDC, addition of 10 μ M purified tPAD1 to the lysate resulted in the activation of FDC, indicating that tPAD catalyzes the conversion of a small molecule in the cell lysate to the cofactor for FDC. Interestingly, in this experiment, purified tPAD alone was quite effective at activating FDC in the absence of cell lysate. This suggests that during purification some of the cofactor remained bound and subsequently diffused from the enzyme. The activation of FDC is not due to FMN diffusing from tPAD1, as FMN itself does not activate FDC (data not shown).

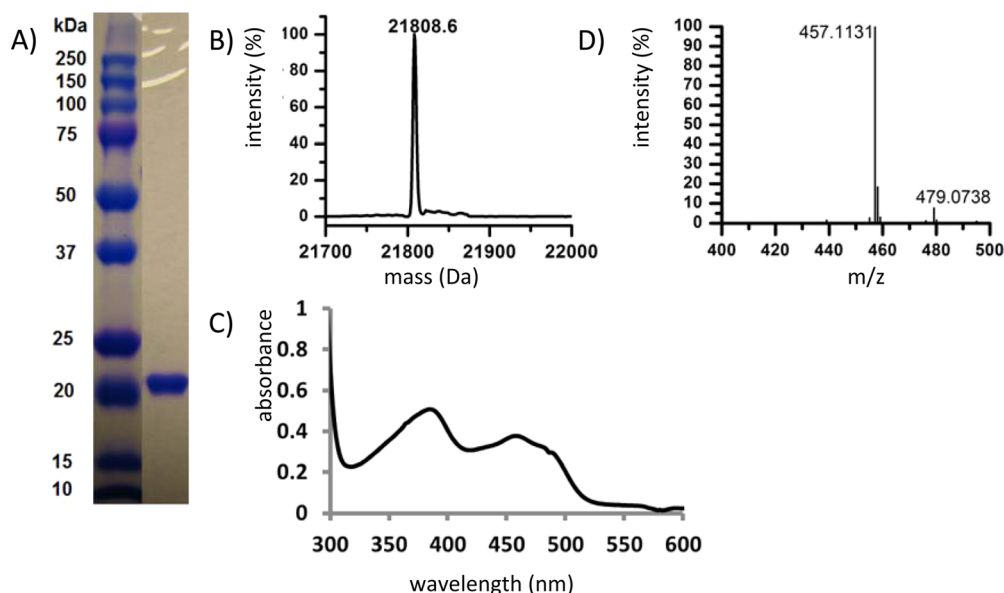


Figure 5. Purification and initial characterization of tPAD1. (A) SDS-PAGE analysis of purified tPAD1. (B) ESI-MS of purified tPAD1. (C) UV-visible spectrum of tPAD1 indicative of bound flavin cofactor(s). LS-MS of flavin cofactor isolated from tPAD1, demonstrating the protein contains FMN.

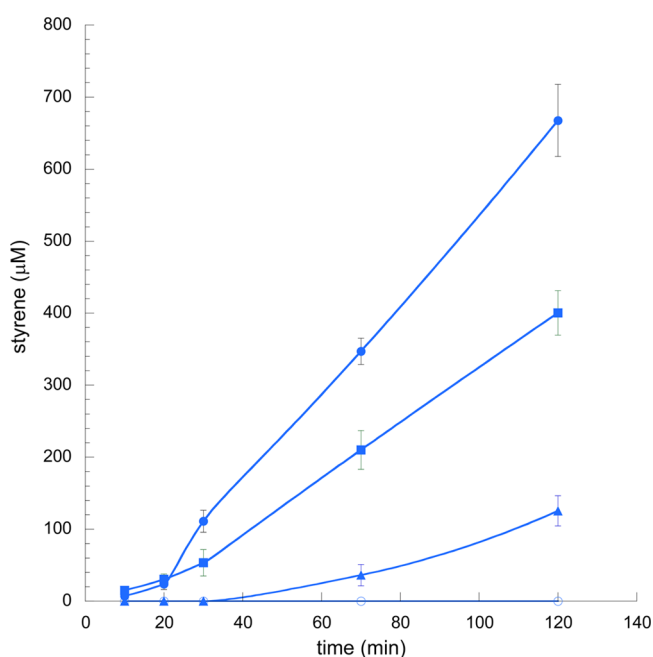


Figure 6. Interaction of tPAD1 and FDC is not required for activation of FDC. 1 μM FDC in buffer containing 6.7 mM cinnamic acid was separated from the other components of the experiment by a 3.5 kDa cutoff dialysis membrane, and the production of styrene was monitored as a function of time. The components added to the other side of the membrane were (○) *E. coli* BL21/ ΔubiX cell lysate; (▲) *E. coli* BL21 cell lysate; (■) purified tPAD1, 10 μM ; (●) *E. coli* BL21/ ΔubiX cell lysate and tPAD1, 10 μM .

Surprisingly, we were unable to detect the presence of the cofactor by LC-ESI-MS (see discussion below) in samples of tPAD1. The reason for this is unclear. It is possible that this reflects the low occupancy of the cofactor in the active site of tPAD1, as a high concentration tPAD1 relative to FDC was used in the dialysis experiments.

Initial Characterization of the FDC Cofactor. The experiments described above suggested that only a small fraction of FDC isolated from *E. coli* BL21 contained the cofactor. Therefore, we attempted to obtain FDC with a higher fraction of cofactor bound by coexpressing FDC with tPAD1 lacking a his-tag in *E. coli* BL21 cells. The specific activity of FDC purified from these cells was much higher: $4.3 \pm 0.2 \mu\text{mol styrene} \cdot \text{min}^{-1} \cdot \text{mg}^{-1}$ enzyme, or ~ 8 -fold higher than that of preparations of FDC from *E. coli* lacking tPAD1. Furthermore, the increased cofactor content resulted in an enzyme preparation that was visibly a pale yellow color. The UV-visible spectrum of the FDC-bound chromophore exhibited an absorbance maximum at 342 nm characteristic of a reduced flavin^{24,25} (Figure 7). However, whereas reduced flavins are readily reoxidized under the aerobic conditions in which the protein was handled,²⁶ the chromophore associated with FDC was stable and its spectrum remained unchanged when it was released from the protein by denaturation with 1:1 dichloromethane/methanol. A preparation of the cofactor, obtained by precipitation of the protein with 1:1 dichloromethane/

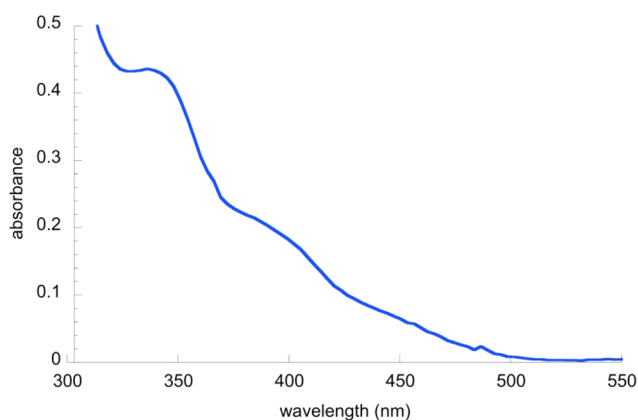


Figure 7. UV-visible spectrum of holo-FDC. The spectrum is suggestive of a reduced flavin-like chromophore.

methanol, followed by removal of the organic solvent was capable of activating apo-FDC, thereby confirming that the yellow chromophore associated with FDC is indeed responsible for the activity of the enzyme.

The protein-free cofactor was further subjected to LC-ESI-MS-MS analysis. The major species in the primary MS spectrum (Figure 8) was characterized a $(M+H^+)/z =$

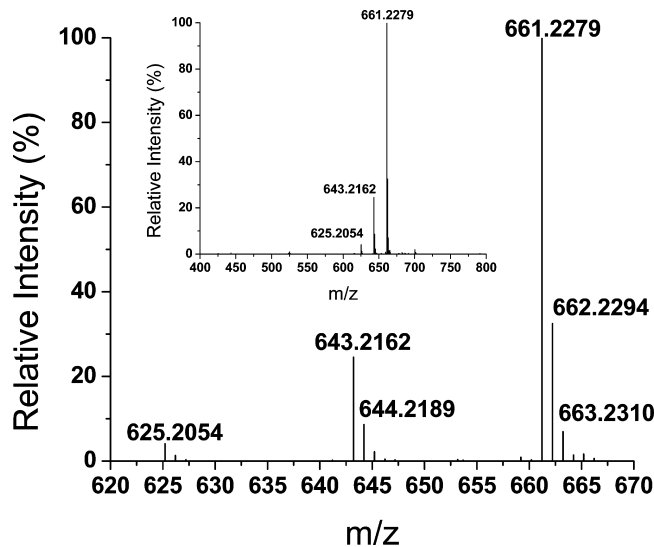


Figure 8. High resolution of ESI-MS spectrum of the novel cofactor for FDC. The less abundant peaks at $(m+1)/z = 643.2162$ and $(m+1)/z = 625.2054$ most likely represent the loss of one and two water molecules from the most abundant species with $(m+1)/z = 661.2279$. Inset: the same spectrum showing a wider spectral window.

661.2212 ± 0.0132 , with minor peaks of $(m+1)/z = 643.2162$ and $(m+1)/z = 625.2054$ that probably represent the loss of one and two water molecules respectively from the parent ion. From this a molecular weight of the cofactor was deduced to be 660.2212 ± 0.0132 . The experimentally determined molecular weight, together with the intensity of the natural abundance ^{13}C peak, is consistent with a molecule possessing between 27–32 carbon atoms. We cautiously note that we cannot definitively rule out, given its labile nature, that this species might represent a fragment of the cofactor. The major $(m/z = 661)$ ion was subjected to fragmentation and attempts were made to match the resulting MS-MS data with various databases of small molecules including Chemical Entities of Biological Interest (ChEBI),²⁷ the Kyoto Encyclopedia of Genes and Genomes (KEGG)²⁸ metabolomics database, the SciFinder (Chemical Abstracts Service) database, and the METLIN²⁹ metabolomics database. However, no convincing matches to compounds in these databases were found. Further attempts to determine the identity of the FDC cofactor were hindered by the small amounts of material available and the instability of the molecule, which appears to lose activity upon release from the enzyme. Although the cofactor retained activity under the mildly acid conditions used in the LC analysis (0.1% formic acid), more strongly acidic (0.1 M HCl for 1 h) or basic (0.1 M NaOH for 1 h) conditions, followed by neutralization, resulted in the loss of activity. LC-MS analysis of acid-treated samples revealed a complex mixture of products that could not be interpreted (data not shown). However, LC-MS analysis of base-treated samples revealed, among other fragments, the presence of a peak with $(m+H^+)/z$

$= 457.1$ corresponding to FMN, providing further evidence that the cofactor comprises a modified form of FMN.

Interestingly, the structures of *E. coli* UbiD,³⁰ a homologous enzyme to FDC, and an UbiD-like protein from *Pseudomonas aeruginosa*¹⁵ have been solved; however, no cofactors are present in the crystal structures. Although the *E. coli* enzyme is a hexamer whereas the *P. aeruginosa* enzyme is dimeric, they have very similar tertiary structures, and it is likely that FDC adopts a similar tertiary structure. The UbiD enzymes comprise three domains, and it is particularly intriguing that the central domain possesses a split β -barrel fold characteristic of flavin-reductases.¹⁵ The structures reveal a large cleft in the putative flavin-binding domain that could potentially accommodate FMN or a modified FMN derivative. We speculate that under the conditions used to overexpress these enzymes for crystallographic analysis, endogenous UbiX could not synthesize sufficient cofactor to saturate UbiD and that the cofactor may also have been lost or degraded during purification. The unavailability of the substrate of these enzymes, 4-hydroxy-3-octaprenylbenzoic acid, prevented their assay to determine whether they were active.

Based on the UV–visible spectrum and its molecular weight, together the fact that PAD1 contains FMN and that FDC resembles other flavin-binding enzymes, we propose that the novel cofactor is likely a modified form of reduced FMN. The fact that the cofactor is stable to air suggests that it is modified at N5, as alkylation on nitrogen would stabilize the reduced flavin ring against reoxidation. Determination of the cofactor's structure presents the next challenge to understanding the reactions catalyzed by PAD1 and FDC. This will likely require the production of isotopically labeled material to facilitate NMR experiments or alternatively could be accomplished if the X-ray structures of holo-FDC or holo-UbiD could be solved.

Steady State Kinetic Properties of FDC. The significant improvement in the activity of FDC resulting from its coexpression with tPAD1 allowed the decarboxylation of cinnamic acid to be followed spectrophotometrically by the decrease in absorbance at 304 nm. Although this limited the upper concentration range of substrate that could be studied before the substrate absorbance became too high, this assay, being far less cumbersome than the GC-MS-based assay, made it feasible to determine k_{cat} and K_{m} for cinnamic acid and the structurally related compounds ferulic acid (*trans*-(4-hydroxy-3-methoxy-phenyl)-acrylic acid) and *p*-coumaric acid (*trans*-(4-hydroxyphenyl)-acrylic acid). The kinetic constants for these substrates, at pH 7.0 and 25 °C in 100 mM potassium phosphate buffer, are given in Table 1.

Although cinnamic acid proved to be the most active substrate, FDC decarboxylated the phenolic substrates, ferulic and coumaric acids, only slightly less efficiently. This suggests that it may be active with a wider range of substituted phenylacrylic acid derivatives, which may lend it to industrial

Table 1. Steady State Kinetic Parameters for FDC

substrate	$k_{\text{cat (app)}} \text{ (s}^{-1}\text{)}^a$	$K_{\text{m}} \text{ (}\mu\text{M)}$	$k_{\text{cat (app)}}/K_{\text{m}} \text{ (s}^{-1}\text{M}^{-1}\text{)}$
cinnamic acid	4.6 ± 0.2	180 ± 24	25500 ± 3500
ferulic acid	3.8 ± 0.3	180 ± 41	21000 ± 4500
coumaric acid	1.5 ± 0.1	110 ± 26	13600 ± 880

^a $k_{\text{cat (app)}}$ values were calculated based on the concentration of FDC protein. As discussed in the text the true k_{cat} is likely significantly higher due to incomplete cofactor occupancy.

uses. Although coexpression of FDC with tPAD1 results in a large increase in enzyme activity, it appears that the cofactor occupancy is still only 20–25% of active sites, assuming that the extinction coefficient for the FDC cofactor is similar to that for reduced FMN. Therefore, the true k_{cat} values for FDC acting on these substrates is most likely 4–5 fold higher than the values reported here.

We note that ferulic acid decarboxylases, also described as phenolic acid decarboxylases, have been described from a variety of bacteria, for example, *Pseudomonas fluorescens* and *Bacillus subtilis*.^{31,32} However, these enzymes require no organic cofactors and are dimers of subunit $M_r = 20$ kDa. They catalyze the decarboxylation of phenolic acids, such as coumaric and ferulic acids, through a mechanism involving deprotonation of the phenolic group to generate a quinone-methide intermediate. However, they do *not* catalyze the decarboxylation of cinnamic acid, in which the phenyl ring is unactivated. The two classes of FDC enzymes are therefore mechanistically quite distinct from each other.

Conclusions. The function of PAD1 and FDC as enzymes involved in the detoxification of aromatic carboxylic acids was first elucidated through genetic analysis of yeast mutants deficient in the metabolism of cinnamic acid and its derivatives.^{9–11} Homologues of these genes are also present in a range of bacteria that have been shown to decarboxylate ferulic and coumaric acids.³³ Although sequence similarities with better-characterized enzymes from other organisms allowed some predictions as to the structure and cofactor requirements of these enzymes to be made, the function of PAD1, which is widely distributed in microbes, has remained confusing. Thus, *E. coli* strains overexpressing the PAD1 gene are unable to decarboxylate phenylacrylic acid derivatives⁸ and the homologue of PAD1 from the enterohemorrhagic *E. coli* strain O157:H7, which has been overexpressed and purified, also exhibited no decarboxylase activity with various phenylacrylic acid derivatives.¹⁶ These observations made it apparent that PAD1 is miss-named as a phenylacrylic acid decarboxylase; however, its actual function remained obscure.

The experiments reported here, which to our knowledge constitute the first time PAD1 and FDC have been biochemically characterized, have clarified the function of PAD1 by showing that it synthesizes a cofactor required by FDC for decarboxylase activity. Although the lability of the cofactor has so far prevented us from determining its structure, based on its UV–visible spectrum, its molecular weight, and the resemblance of PAD1 and FDC to other flavin-binding enzymes, we propose that the cofactor is likely a new, modified form of reduced FMN. In the absence of a structure, the mechanism by which the cofactor facilitates the decarboxylation of cinnamic acid remains a mystery, as this type of decarboxylation reaction appears to lack any obvious precedent in flavo-protein chemistry.

PAD1 and FDC share sequence similarities with the *E. coli* enzymes UbiX and UbiD, which are involved in decarboxylation of 4-hydroxy-3-octaprenylbenzoic acid, an early step ubiquinone biosynthesis. (We note that yeast, being eukaryotes, synthesize ubiquinone by a slightly different pathway³⁴ and that PAD1 and FDC are not involved in ubiquinone biosynthesis.) We have shown that UbiX can replace PAD1 in activating FDC and it was previously shown that PAD1 restores ubiquinone biosynthesis in a ΔubiX *E. coli* strain. Therefore, UbiX and PAD1 appear to be isofunctional enzymes. This strongly suggests that UbiD is, in fact, the 4-hydroxy-3-octaprenylben-

zoic acid decarboxylase and that it uses the same cofactor as FDC. The existence of Pad1p, distinct from UbiX, in some *E. coli* strains is intriguing as it suggests further biological roles for this novel cofactor.

METHODS

Plasmid and Strain Construction. A derivative strain of *E. coli* BL21 in which the *ubiX* gene was deleted was obtained by P1 phage transduction as previously described.^{35,36} The P1 phage lysate was prepared from the Keio single gene knockout strain $\Delta\text{ubiX}::\text{kan}$ and used to transduce the *ubiX* knockout into *E. coli* BL21 Star (DE3) to obtain a strain designated *E. coli* BL21/ ΔubiX .

The genes encoding FDC (YDR539W) and PAD1 (YDR538W) from *S. cerevisiae* were synthesized commercially by GenScript U.S.A. Inc. (Piscataway, NJ, U.S.A.) and codon-optimized for expression in *E. coli*. The synthetic genes FDC and PAD1 were subcloned into the expression vector pET-28b utilizing the *NdeI* and *BamHI* restriction sites to generate plasmids pFDC and pPAD1. This introduced a vector-encoded N-terminal 6 histidine-tag to facilitate enzyme purification. For protein expression, the plasmids were transformed into the *E. coli* strains BL21 (DE3) (Invitrogen) and *E. coli* BL21/ ΔubiX .

To delete the N-terminal mitochondrial targeting peptide sequence (residues 1–58) from PAD1 a truncated gene was constructed by PCR using the following oligonucleotides as the forward (5'-TAACATATGAAACGTATTGTGGTTGCGAT-3') and reverse primers (5'-AGTGGATCCTTATTTTATTGATTTGATACCTTCCC-3') and pPAD1 as the template. After amplification, the PCR product was digested with *NdeI* and *BamHI* and ligated with pET28b linearized with *NdeI* and *BamHI*. The resulting plasmid, ptPAD1 was transformed into *E. coli* BL21 (DE3) for expression of tPAD1.

For the coexpression of tPAD1 and FDC the two genes were introduced in tandem into pET28b and expressed from a single vector-encoded promoter. The tPAD1 gene was amplified by PCR using forward primer (5'-ATTCCATGGGCAAACGTATTGTGGTTGCGAT-3') and reverse primer (5'-AGTGGATCCTTATTTTATTGATTTGATACCTTCCC-3') using pPAD1 as the template. After amplification, the PCR product was digested with *NcoI* and *BamHI* and ligated with pET28b linearized with *NcoI* and *BamHI*. The resulting plasmid, ptPAD1nohis lacks an encoded N-terminal His tag. The FDC gene was introduced behind the tPAD1 gene and the stop codon deleted to allow for the incorporation of a C-terminal vector-encoded 6 histidine tag. This was accomplished by PCR using the forward primer (5'-ATTGAGCTCGAAGTATAAGAAGGAGATATATTCATGCGCAAACCTGAACCCGG-3') which introduced a ribosome binding sequence, shown in bold, and the reverse primer (5'-AATGTCGACTTTGTAACCGTAGCGTTTCCAGTTTTCATT-3') and using pFDC as the template. The PCR product was digested with *SacI* and *SalI* and ligated with ptPAD1nohis cut with *SacI* and *SalI* to produce ptPAD1-FDC, which was transformed into *E. coli* BL21 (DE3) to coexpress both tPAD1 and FDC genes.

Enzyme Expression and Purification. Protein expression was performed by standard methods. *E. coli* cultures were grown at 32 °C in LB medium supplemented with 50 $\mu\text{g}/\text{mL}$ kanamycin to an OD_{600} of 0.6–0.8 and gene expression induced with 0.2 mM isopropyl- β -thiogalactopyranoside (IPTG) overnight before harvesting the cells by centrifugation.

In a typical purification of FDC or PAD1, 7 g (damp weight) of cells were resuspended in 50 mL binding buffer (20 mM phosphate buffer, pH 8.0, 500 mM NaCl, 20 mM imidazole, 5% glycerol, 1 mM THP). 0.5 mg mL^{-1} of lysozyme, 1 protease inhibitor tablet (Roche), 1 μL of DNase (Novagen), and 1 mM tris(hydroxylpropyl) phosphine (THP) were added to the cell suspension and incubated on ice for 1 h with gentle shaking. The cells were lysed by sonication at maximum power using 2 s pulses separated by 8 s to prevent overheating for a total time of 30 min. The supernatant was separated from cell debris by centrifugation at 15000g at 4 °C for 30 min. Protein purification was performed using an ÄKTAexplorer chromatography system. The supernatant was loaded onto a HisTrap column (GE Healthcare) and

the column was washed with buffer (20 mM phosphate buffer, pH 8.0, containing 500 mM NaCl, 60 mM imidazole, 5% glycerol) at a flow rate of 1.0 mL/min. The enzyme was eluted from the column with 500 mM imidazole in the same buffer. The resulting fractions were analyzed by SDS-PAGE on a 15% gel. The fractions containing pure protein were pooled and passed through PD-10 column (GE Healthcare) for desalting into PBS buffer plus 5% glycerol.

GC-MS Enzyme Assay. Routine assays of FDC activity were carried out in PBS buffer, pH 8.0, with a total volume of 500 μ L, using a saturating concentration of cinnamic acid, 6.7 mM, as the substrate; the concentration of FDC was typically 1.0 μ M. Assays utilizing tPAD1 typically included this enzyme at 10 μ M concentration. The assay mixtures were incubated at 32 °C for varying lengths of time, after which the reaction was quenched and the reaction products were extracted by addition of 500 μ L ethyl acetate; samples were vortexed for 15 min and then centrifuged in a microfuge at 12000 rpm for 20 min to separate the organic and aqueous phases. The amount of styrene produced was determined by GC-MS. For assays in which the pH was varied, assays containing 6.7 mM cinnamic acid and 1 μ M FDC were incubated at 32 °C for 10 min. The styrene produced was then extracted with ethyl acetate and the concentration of styrene was determined by GC-MS. Control experiments were undertaken to ensure that the substrate concentration remained saturating throughout the pH range.

GC-MS analysis was performed using a Shimadzu QP-2010S GC-MS instrument equipped with a quadrupole mass detector and a DB-5 column (Restek, 30m \times 0.25 mm \times 0.25 μ m). The flow rate of the helium carrier gas is constant at 1 mL/min and the inlet temperature was maintained at 200 °C. The interface temperature was maintained at 250 °C. Injections (10 μ L) of the ethyl acetate extracted were made in splitless mode. The oven temperature was held initially at 40 °C for 3.5 min, gradually increased to 90 °C at 14 °C/min, then gradually increased from 90 to 315 °C at 20 °C/min, and, finally, maintained at 315 °C for 1 min. Chromatographic data were analyzed by GC-MS PostRun analysis software. Enzymatic conversion of cinnamic acid to styrene was quantified using a calibration plot of styrene standards of known concentration.

Spectroscopic Enzyme Assay. For high activity preparations of FDC, that is, enzyme prepared from *E. coli* strains coexpressing tPAD1, the decarboxylation of substrates could be followed by the decrease in absorbance of the UV-active substrates. Typical assays were performed in 100 mM potassium phosphate buffer, pH 7.0, at room temperature (RT) and contained 250–500 nM FDC. The substrate concentrations ranged between 0.05 mM and 1.5 mM; at higher concentrations, the absorbance of the substrate became too high. Decarboxylase activity was followed by monitoring the decrease in absorbance at 304 nm for cinnamic acid $\epsilon_0 = 1140 \text{ M}^{-1}\text{cm}^{-1}$; 334 nm for para-coumeric acid $\epsilon_0 = 988 \text{ M}^{-1}\text{cm}^{-1}$; and 344 nm for ferulic acid $\epsilon_0 = 1330 \text{ M}^{-1}\text{cm}^{-1}$. Velocity data were fitted to the Michaelis–Menten equation using Origin software.

LC-MS Analysis of Proteins and Small Molecules. The molecular weights of proteins and small molecules were determined using an Agilent 6520 LC-accurate-mass Q-TOF MS system. The protein was passed through a desalting column and acidified with 0.1% formic acid. The sample (5 μ L) was injected onto a Poroshell 300SB-C8 column equilibrated with 0.1% formic acid and 5% acetonitrile. Proteins were eluted for 5 min with 95% water: 5% acetonitrile followed by an increasing gradient of acetonitrile to 100% over 7 min at a flow rate of 0.5 mL/min. Eluting proteins were detected at 280 nm. Mass data were obtained using intact protein mode and analyzed using Agilent MassHunter Qualitative Analysis software. The raw data was deconvoluted with respect to maximum entropy. For small molecule analysis, proteins were precipitated with an equal volume of 1:1 dichloromethane/methanol in glass tubes and removed by centrifugation at 3000g for 10 min. The organic solvent was removed under a stream of nitrogen. The sample (20 μ L) then was injected onto a Zorbax 300SB-C18 column equilibrated with 0.1% formic acid and 5% acetonitrile, followed by a 2 min washing with 95% water/5% acetonitrile. Then, the gradient of acetonitrile was increased to 100% over 10 min at a flow rate of 0.4 mL/min. Mass data were obtained

using small molecular mode and analyzed using Agilent MassHunter Qualitative Analysis software. MS/MS data was obtained by automatic MS/MS acquisition. A continuous scan event consisting of one full MS scan (50–2000 m/z) followed by three data-dependent MS/MS scans were carried out. The three most intense ions from the initial MS scan were selected individually for collision-induced dissociation at 50 eV.

AUTHOR INFORMATION

Corresponding Authors

*E-mail: nmarsh@umich.edu.

*E-mail: ninalin@umich.edu.

Present Address

^{||}State Key Laboratory of Bioelectronics, School of Biological Science and Medical Engineering, Southeast University, Nanjing 210096, China.

Notes

The authors declare no competing financial interest.

ACKNOWLEDGMENTS

This research was supported in part by grants from the National Science Foundation, CHE 1152055 (to E.N.G.M.) and CBET 1336636 (to E.N.G.M. and X.N.L.). F.L. is a recipient of a PISET fellowship from the University of Michigan Energy Institute. We thank Dr. Stephen Brown of the University of Michigan Metabolomics Core Services supported by grant U24 DK097153 of the National Institutes of Health (NIH) Common Funds Project to the University of Michigan for LC-MS analyses of cofactor samples.

REFERENCES

- (1) Cleland, W. W. (1999) Mechanisms of enzymatic oxidative decarboxylation. *Acc. Chem. Res.* 32, 862–868.
- (2) Jordan, F., and Patel, H. (2013) Catalysis in enzymatic decarboxylations: Comparison of selected cofactor-dependent and cofactor-independent examples. *ACS Catal.* 3, 1601–1617.
- (3) Belcher, J., McLean, K. J., Matthews, S., Woodward, L. S., Fisher, K., Rigby, S. E. J., Nelson, D. R., Potts, D., Baynham, M. T., Parker, D. A., Leys, D., and Munro, A. W. (2014) Structure and biochemical properties of the alkene producing cytochrome P450 OleTJE (CYP152L1) from the *Jeotgaliococcus* sp. 8456 bacterium. *J. Biol. Chem.* 289, 6535–6550.
- (4) Kourist, R., Guterl, J.-K., Miyamoto, K., and Sieber, V. (2014) Enzymatic decarboxylation—An emerging reaction for chemicals production from renewable resources. *ChemCatChem* 6, 689–701.
- (5) Straathof, A. J. J. (2014) Transformation of biomass into commodity chemicals using enzymes or cells. *Chem. Rev.* 114, 1871–1908.
- (6) Shin, J. H., Kim, H. U., Kim, D. I., and Lee, S. Y. (2013) Production of bulk chemicals via novel metabolic pathways in microorganisms. *Biotechnol. Adv.* 31, 925–935.
- (7) Jung, D.-H., Choi, W., Choi, K.-Y., Jung, E., Yun, H., Kazlauskas, R. J., and Kim, B.-G. (2013) Bioconversion of p-coumaric acid to p-hydroxystyrene using phenolic acid decarboxylase from *B. amyloliquefaciens* in biphasic reaction system. *Appl. Microbiol. Biotechnol.* 97, 1501–1511.
- (8) McKenna, R., and Nielsen, D. R. (2011) Styrene biosynthesis from glucose by engineered *E. coli*. *Metab. Eng.* 13, 544–554.
- (9) Mukai, N., Masaki, K., Fujii, T., Kawamukai, M., and Iefuji, H. (2010) PAD1 and FDC1 are essential for the decarboxylation of phenylacrylic acids in *Saccharomyces cerevisiae*. *J. Biosci. Bioeng.* 109, 564–569.
- (10) Clausen, M., Lamb, C. J., Megnet, R., and Doerner, P. W. (1994) *Pad1* encodes phenylacrylic acid decarboxylase which confers resistance to cinnamic acid in *Saccharomyces cerevisiae*. *Gene* 142, 107–112.

- (11) Stratford, M., Plumridge, A., and Archer, D. B. (2007) Decarboxylation of sorbic acid by spoilage yeasts is associated with the *PAD1* gene. *Appl. Environ. Microbiol.* **73**, 6534–6542.
- (12) Bentinger, M., Tekle, M., and Dallner, G. (2010) Coenzyme Q—Biosynthesis and functions. *Biochem. Biophys. Res. Commun.* **396**, 74–79.
- (13) Gulmezian, M., Hyman, K. R., Marbois, B. N., Clarke, C. F., and Javor, G. T. (2007) The role of UbiX in *Escherichia coli* coenzyme Q biosynthesis. *Arch. Biochem. Biophys.* **467**, 144–153.
- (14) Zhang, H. T., and Javor, G. T. (2003) Regulation of the isofunctional genes *ubiD* and *ubiX* of the ubiquinone biosynthetic pathway of *Escherichia coli*. *FEMS Microbiol. Lett.* **223**, 67–72.
- (15) Jacewicz, A., Izumi, A., Brunner, K., Schnell, R., and Schneider, G. (2013) Structural insights into the UbiD protein family from the crystal structure of PA0254 from *Pseudomonas aeruginosa*. *PLoS One* **8**, e63161.
- (16) Rangarajan, E. S., Li, Y. G., Iannuzzi, P., Tocili, A., Hung, L. W., Matte, A., and Cygler, M. (2004) Crystal structure of a dodecameric FMN-dependent UbiX-like decarboxylase (Pad1) from *Escherichia coli* O157:H7. *Protein Sci.* **13**, 3006–3016.
- (17) Kopec, J., Schnell, R., and Schneider, G. (2011) Structure of PA4019, a putative aromatic acid decarboxylase from *Pseudomonas aeruginosa*. *Acta Crystallogr., Sect. F: Struct. Biol. Cryst. Commun.* **67**, 1184–1188.
- (18) Blaesse, M., Kupke, T., Huber, R., and Steinbacher, S. (2000) Crystal structure of the peptidyl-cysteine decarboxylase EpiD complexed with a pentapeptide substrate. *EMBO J.* **19**, 6299–6310.
- (19) Blaesse, M., Kupke, T., Huber, R., and Steinbacher, S. (2003) Structure of MrsD, an FAD-binding protein of the HFCD family. *Acta Crystallogr. Sect. D: Biol. Crystallogr.* **59**, 1414–1421.
- (20) Majer, F., Schmid, D. G., Altena, K., Bierbaum, G., and Kupke, T. (2002) The flavoprotein MrsD catalyzes the oxidative decarboxylation reaction involved in formation of the peptidoglycan biosynthesis inhibitor mersacidin. *J. Bacteriol.* **184**, 1234–1243.
- (21) Strauss, E., and Begley, T. P. (2001) Mechanistic studies on phosphopantothenoylcysteine decarboxylase. *J. Am. Chem. Soc.* **123**, 6449–6450.
- (22) Strauss, E., Kinsland, C., Ge, Y., McLafferty, F. W., and Begley, T. P. (2001) Phosphopantothenoylcysteine synthetase from *Escherichia coli*—Identification and characterization of the last unidentified coenzyme A biosynthetic enzyme in bacteria. *J. Biol. Chem.* **276**, 13513–13516.
- (23) Kupke, T. (2002) Molecular characterization of the 4'-phosphopantothenoylcysteine synthetase domain of bacterial Dfp flavoproteins. *J. Biol. Chem.* **277**, 36137–36145.
- (24) Ghisla, S., and Massey, V. (1989) Mechanisms of flavoprotein-catalyzed reactions. *Eur. J. Biochem.* **181**, 1–17.
- (25) Fraaije, M. W., and Mattevi, A. (2000) Flavoenzymes: Diverse catalysts with recurrent features. *Trends Biochem. Sci.* **25**, 126–132.
- (26) Massey, V. (1994) Activation of molecular-oxygen by flavins and flavoproteins. *J. Biol. Chem.* **269**, 22459–22462.
- (27) de Matos, P., Alcantara, R., Dekker, A., Ennis, M., Hastings, J., Haug, K., Spiteri, I., Turner, S., and Steinbeck, C. (2010) Chemical entities of biological interest: An update. *Nucleic Acids Res.* **38**, D249–D254.
- (28) Kanehisa, M., Araki, M., Goto, S., Hattori, M., Hirakawa, M., Itoh, M., Katayama, T., Kawashima, S., Okuda, S., Tokimatsu, T., and Yamanishi, Y. (2008) KEGG for linking genomes to life and the environment. *Nucleic Acids Res.* **36**, D480–D484.
- (29) Smith, C. A., O'Maille, G., Want, E. J., Qin, C., Trauger, S. A., Brandon, T. R., Custodio, D. E., Abagyan, R., and Siuzdak, G. (2005) METLIN—A metabolite mass spectral database. *Ther. Drug Monit.* **27**, 747–751.
- (30) Zhou, W., Forouhar, F., Seetharaman, J., Fang, Y., Xiao, R., Cunningham, K., Ma, L. C., Chen, C. X., Acton, T. B., Montelione, G. T., Hunt, J. F., and Tong, L. (2006) Crystal structure of 3-octaprenyl-4-hydroxybenzoate decarboxylase (UbiD) from *Escherichia coli*, Northeast Structural Genomics target ER459. *Protein Data Bank*, DOI: 10.2210/pdb2idb/pdb.
- (31) Huang, Z. X., Dostal, L., and Rosazza, J. P. N. (1994) Purification and characterization of a ferulic acid decarboxylase from *Pseudomonas fluorescens*. *J. Bacteriol.* **176**, 5912–5918.
- (32) Cavin, J. F., Dartois, V., and Divies, C. (1998) Gene cloning, transcriptional analysis, purification, and characterization of phenolic acid decarboxylase from *Bacillus subtilis*. *Appl. Environ. Microbiol.* **64**, 1466–1471.
- (33) Barthelmebs, L., Divies, C., and Cavin, J. F. (2000) Knockout of the p-coumarate decarboxylase gene from *Lactobacillus plantarum* reveals the existence of two other inducible enzymatic activities involved in phenolic acid metabolism. *Appl. Environ. Microbiol.* **66**, 3368–3375.
- (34) Meganathan, R. (2001) Ubiquinone biosynthesis in microorganisms. *FEMS Microbiol. Lett.* **203**, 131–139.
- (35) Baba, T., Ara, T., Hasegawa, M., Takai, Y., Okumura, Y., Baba, M., Datsenko, K. A., Tomita, M., Wanner, B. L., and Mori, H. (2006) Construction of *Escherichia coli* K-12 in-frame, single-gene knockout mutants: The Keio collection. *Mol. Syst. Biol.* **2**, 2006.0008.
- (36) Miller, J. H. (1992) *A Short Course in Bacterial Genetics: A Laboratory Manual and Handbook for Escherichia coli and Related Bacteria*; Cold Spring Harbor Laboratory Press, Plainview, NY.